Applied Physics Letters

Electric field dependent polarization switching of tetramethylammonium bromotrichloroferrate(III) ferroelectric plastic crystals

Cite as: Appl. Phys. Lett. **116**, 242902 (2020); https://doi.org/10.1063/5.0004387
Submitted: 10 February 2020 . Accepted: 28 May 2020 . Published Online: 15 June 2020

Julian Walker, Simon Scherrer, Nora Statle Løndal, Tor Grande, and Mari-Ann Einarsrud

Applied Physics Letters ARTICLE scitation.org/journal/apl

Electric field dependent polarization switching of tetramethylammonium bromotrichloroferrate(III) ferroelectric plastic crystals

Cite as: Appl. Phys. Lett. **116**, 242902 (2020); doi: 10.1063/5.0004387
Submitted: 10 February 2020 · Accepted: 28 May 2020 ·
Published Online: 15 June 2020

Julian Walker,[a] Simon Scherrer, Nora Statle Løndal, Tor Grande, and Mari-Ann Einarsrud

AFFILIATIONS

Department of Materials Science and Engineering, NTNU Norwegian University of Science and Technology, Trondheim N-7491, Norway

[a]Author to whom correspondence should be addressed: julian.walker@ntnu.no

ABSTRACT

Tetramethylammonium bromotrichloroferrate(III) ($[N(CH_3)_4][FeBrCl_3]$) is a plastic crystal ferroelectric with small dielectric constant <20 and piezoelectric coefficient as high as 110 pC/N. Here, super-coercive hysteresis and dielectric properties under direct current (DC) bias fields up to 260 and 120 kV/cm, respectively, were studied to shed light on the polarization switching $[N(CH_3)_4][FeBrCl_3]$ and the related family of plastic crystal and supramolecular ferroelectrics. $[N(CH_3)_4][FeBrCl_3]$ exhibited peak-to-peak strains of 0.1% and saturated ferroelastic switching at fields of 170 kV/cm. Above 170 kV/cm, rates of field increase were too fast for domain switching, resulting in reduced strain rates during the switching cycle. Leakage currents had larger contributions at higher field amplitudes. This was also reflected in the switching behavior at higher frequencies, 100 Hz, in which hysteresis was asymmetric and switching incomplete. The dielectric constant and loss exhibited a butterfly-like shape during application of DC bias electric fields indicative of domain switching, but showed a small dielectric tunability of 0.038 and no signs of dielectric stiffening, with the relative permittivity from 16.9 to 17.3 at fields from 0 to 120 kV/cm. The present findings provide insight into the domain switching kinetics and dielectric properties of $[N(CH_3)_4][FeBrCl_3]$ that will assist with further development of plastic crystal ferroelectrics.

Ferroelectric materials with low dielectric constants and high piezoelectric coefficients are uniquely suited for applications like sensing and energy harvesting, where the figure of merit is inversely proportional to the dielectric constant.[1,2] Demand for these applications will increase as the Internet of Things (IoT), smart buildings, self-driven electric vehicles, and energy autonomous devices become more prevalent in society.[3,4] Many commercial ferroelectrics, such as $BaTiO_3$ and $PbZr_{0.52}Ti_{0.48}O_3$ (PZT) however, have high dielectric constants, brittle mechanical properties, and face a number of synthesis challenges, which can make them less than ideal for many applications in this growing area.[1,5] The investigation of materials with small dielectric responses and greater mechanical flexibility, such as supramolecular and organic–inorganic hybrids, is therefore a useful avenue of investigation for the development of alternative sensor and energy harvester devices.[6]

$[N(CH_3)_4][FeBrCl_3]$ is a supramolecular hybrid organic–inorganic plastic crystal that was recently identified with useful dielectric and electromechanical properties, such as a low dielectric constant (relative permittivity <20) and a strong piezoelectric coefficient (d_{33}) of 110 pC/N.[7] $[N(CH_3)_4][FeBrCl_3]$ has a noncentrosymmetric orthorhombic *Amm*2 crystal structure at room temperature [Fig. 1(a)] and four temperature dependent polymorphs between 0 and 110 °C, with a ferroelectric to paraelectric transition between 70 and 90 °C.[7–9] Above 110 °C, the material forms a cubic mesophase, in which the molecular ions rotate freely in the crystal lattice and allow the material to be plastically deformed.[7] The mesophase provides a pathway for low temperature synthesis of polycrystalline materials, making $[N(CH_3)_4][FeBrCl_3]$ appealing from an environmental perspective, and for compatibility with other polymeric materials. Despite the potential of $[N(CH_3)_4][FeBrCl_3]$ and the wider family of plastic crystal ferroelectrics, critical aspects of the ferroelectric properties, such as switching dynamics, electric field dependence, and leakage currents, have not yet been thoroughly characterized. To help rectify this, we report on the characteristics of electric field dependent switching of polycrystalline $[N(CH_3)_4][FeBrCl_3]$.

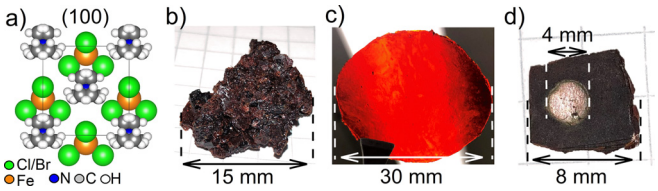

FIG. 1. (a) Model of the $[N(CH_3)_4][FeBrCl_3]$ *Amm*2 crystal structure in the (100) plane, with multiple equivalent positions of different rotation states for carbon and hydrogen. Photographs of (b) crystal agglomerate after drying, (c) after hot pressing, and (d) after cutting and electrode deposition.

Polycrystalline $[N(CH_3)_4][FeBrCl_3]$ was prepared by separately dissolving methylammonium bromide (99%, Sigma Aldrich) and iron trichloride hexahydrate (98%, Sigma Aldrich) in de-ionized water and mixing 1:1 molar ratios of each solution. Crystallization occurred at room temperature during slow evaporation of water over 7 days. Crystals were vacuum filtrated and dried in vacuum at 60 °C for 6 h. The largest crystal agglomerates, averaging 15 mm in diameter [Fig. 1(b)], were hot pressed at 140 °C and 10 MPa into flat 380 μm thick 30 mm diameter disks [Fig. 1(c)]. The disks were cut into 10 mm^2 pieces and sputter coated with 4 mm diameter Au electrodes [Fig. 1(d)]. The whole synthesis process therefore involved only aqueous solvents and temperatures no higher than 140 °C.

The orthorhombic *Amm*2 crystal structure [Fig. 1(a)] was confirmed by x-ray diffraction (XRD) using a D8 focus x-ray diffractometer with a Cu source and Rietveld refinement, fitted to the Cambridge crystallographic data center (CCDC) file 1574204 from Harada *et al.* using the Topas® software package (data not shown). All bipolar electric field hysteresis and dielectric measurements of $[N(CH_3)_4][FeBrCl_3]$ were measured with an *Axiacct* ferroelectric tester, trek 10 kV amplifier, and a laser interferometer. A triangular wave form at a frequency of 10 Hz was used for hysteresis measurements at field amplitudes up to 260 kV/cm. Samples were stored in a desiccator and were typically hot pressed and electroded within one week of their electrical measurements. Measurements conducted several weeks or months after processing confirmed that leakage currents did increase but that ferroelectric behavior was qualitatively comparable. The single most influential factor on electrical leakage was the process of drying of crystals after synthesis. Poorly dried samples, for example, those dried on a hot plate and not in a vacuum oven, had leakage currents orders of magnitude higher. Effects of drying method are discussed in more detail elsewhere.[10]

Polarization–electric field (P–E) loops with field amplitudes from 80 to 260 kV/cm opened significantly as both remnant polarization (P_r) and coercive field (E_c) increased [Fig. 2(a)]. P_r is the polarization at 0 kV/cm and E_c is the electric field at 0 $\mu C/cm^2$, each shown by the dashed arrows [Fig. 2(a)]. The polarization of each loop continued to increase after the maximum electric field was reached, creating a bloated rounded shape of the P–E loops, highlighted by the curved arrows. This demonstrated that significant leakage currents were present at higher field amplitudes.[11] Due to the leakage currents, we employed the term apparent remanent polarization (P_r*) to describe the polarization at 0 kV/cm, as this value includes significant contributions from both leakage current and the remanent polarization of ferroelectric (180°) and ferroelastic (non-180°) domains. The P_r* values reached 5.0 $\mu C/cm^2$ at field amplitudes of 150 kV/cm and nearly 10 $\mu C/cm^2$ at field amplitudes of 260 kV/cm [Fig. 2(a)]. However, P_r of 4 $\mu C/cm^2$ at field amplitudes of 110 kV/cm are reported in the literature and thus, here it is anticipated that leakage currents may contribute to up to 50% of the Pr* value at high fields.[7]

The current density–electric field (I–E) loops also show the presence of strong domain switching and leakage current [Fig. 2(b)].[11,12] The sharp current density peaks are produced by the switching of ferroelectric domains. The peak gives the average E_c and the width of its distribution. The E_c increased with increasing field amplitude, as indicated by the dashed lines [Fig. 2(b)]. After reaching maximum fields, the I–E loops curved nonlinearly as the electric field reduced to 0 kV/cm, highlighted by curved arrows. It is evident from the data that the increased leakage current contributions at higher electric fields.

The electromechanical response was observed by strain–electric field hysteresis (S–E) loops [Fig. 2(c)]. The S–E loops exhibited a butterfly-like shaped strain fingerprint characteristic of electromechanical strain contributions from ferroelastic domain switching, domain wall motion, piezoelectric strain, and electrostriction.[13,14] At 80 kV/cm, the loops had a small peak-to-peak strain (S_{pp}) on the order of 0.014%, but reaching a maximum S_{pp} of 0.109% with increasing field. The E_c from the S–E loops was identified by the strain minima, marked with dashed lines for 80 and 260 kV/cm loops, and increased with field amplitude similarly as with P–E and I–E loops.

Critical parameters of the P–E, I–E, and S–E hysteresis loops were analyzed as a function of the driving electric field amplitude [Figs. 2(d)–2(g)]. The P_r* increased linearly up to 170 kV/cm and the polarization at maximum electric field (E_{max}) increased linearly with two distinct gradients above and below 170 kV/cm [Fig. 2(d)]. The current density peaks (I_{peak}) correspond with the greatest number of domains switching during the electric field cycle, and also exhibited different linear gradients as a function of field amplitude above and below 170 kV/cm [Fig. 2(e)]. The peak-to-peak strain (S_{pp}), which is a measure of the total strain generated during the domain switching, increased from 0.014% to 0.109% between field amplitudes 80 and 170 kV/cm and plateaued at fields above 170 kV/cm [Fig. 2(f)].

Two physical explanations can be used to understand the behavior observed for P_r*, polarization at E_{max}, I_{peak}, and S_{pp}. Below 170 kV/cm, the number of domains being switched for the first time increases with the increasing field amplitude, but above 170 kV/cm, this number decreases with increasing field amplitude.[11–13] The constant S_{pp} above 170 kV/cm indicates that the total number of ferroelastic domains being switched saturates, as only the ferroelastic domains will contribute to strain and there is no direct contribution from leakage current. The smaller gradients seen above 170 kV/cm in P_r*, polarization at E_{max} and I_{peak} all suggested that ferroelectric domain switching may also begin to saturate, but domains and leakage current contributions cannot be separated in these data.

The difference between E_c in positive (E_c^+) and negative (E_c^-) field directions determined from the I–E loop peak positions were plotted together with the internal bias fields ($E_{bias} = E_c^+ - E_c^-$) and indicated preferential switching of domains [Fig. 2(g)].[13,15,16] Both E_c^+ and E_c^- increased with field amplitude at a decreasing rate, while the E_{bias} decreased from 9 to 2 kV/cm between 80 and 170 kV/cm above which it fluctuated. The E_{bias} of $[N(CH_3)_4][FeBrCl_3]$ at lower electric fields suggests the presence of oriented defect complexes [Fig. 2(g)].[16] $V^{\bullet}_{[FeBrCl3]}$ ($[FeBrCl_3]^-$ lattice vacancy in Kröger–Vink notation) and

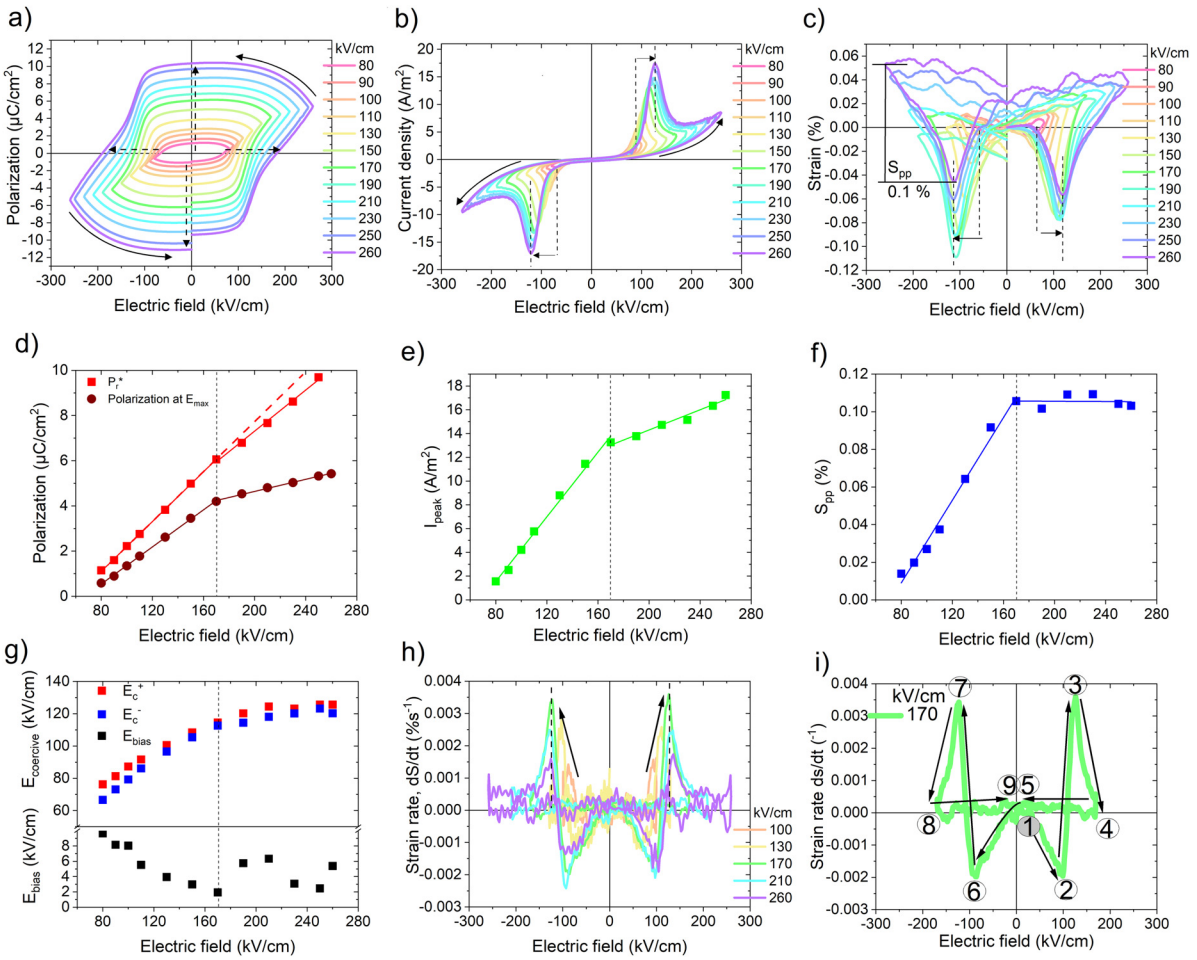

FIG. 2. (a)–(c) Hysteresis loops with an electric field frequency of 10 Hz and field amplitudes from 80 to 270 kV/cm, (a) polarization, dashed arrows show increase in E_c and P_r* and curved arrows indicate leakage contribution. (b) Current density, dashed lines, and straight arrows show movement of E_c and curved arrows show leakage contribution. (c) Strain, dashed lines, and straight arrows show movement of E_c. (d) Apparent remanent polarization (P_r*) and polarization at maximum field (E_{max}). (e) Current density peak magnitude (I_{peak}). (f) Peak-to-peak strain (S_{pp}). (g) Positive (E_c^+) and negative (E_c^-) coercive field and the internal bias field (E_{bias}) determined from (b). Lines in figures (d)–(g) are linear fits for data above and below 170 kV/cm. (h) Strain rate (ds/dt) hysteresis, dashed lines mark the largest rate at 130 kV/cm and the arrows guide the eye along the movement strain rate peaks. (i) Strain rate at 170 kV/cm with arrows showing the loop progression starting at point 1. Key points along the loop are labeled from 1 to 9.

$Br'_{[FeBrCl3]}$ were previously identified as likely charged point defects that could form a complex.[10] Orientation of these defects could result from hot pressing, as complex defects can have both an electrical and mechanical dipole.[17] The reduction of E_{bias} up to 170 kV/cm implies that the preferred orientation was destroyed by the bipolar electric field or that the defects were mobile.[15,16] The instability of the E_{bias} at fields >170 kV/cm may relate to the leakage current.

Strain rate hysteresis curves are a plot of the first derivative of the strain (ds/dt) as a function of electric field, thus the relationship between strain and strain rate is analogous to that of the polarization and current hysteresis [Fig. 2(g)].[14] Among other useful features, the peaks in the strain rate signify where the largest amount of ferroelastic domain reorientation took place during an electric field cycle. To understand the strain rate hysteresis of $[N(CH_3)_4][FeBrCl_3]$ in terms of switching kinetics, we first analyzed the loop with field amplitude 170 kV/cm [Fig. 2(i)]. The strain rate hysteresis at 170 kV/cm was highly symmetrical with a total of four distinct peaks corresponding to inflection points of the S–E loops. The strain loop had two minima and two maxima, indicating two consecutive and reproducible steps of ferroelastic domain switching in each field direction.[14] Notably, the strain rate hysteresis loops bore significant qualitative similarities to that of commercial soft PZT ceramics (PZT 5H) and so an over simplified model of domain switching with domains approximately parallel, perpendicular, and anti-parallel to the electric field (as if the structure had tetragonal symmetry) was useful to qualitatively describe the two-step switching process.

As the electric field first increased the material shrank, indicated by the negative strain rate [points 1–2, Fig. 2(i)]. This was associated with depoling the sample from the remanent polarization state left by the previous electric field cycle.[14] The shrinkage rate reached a sharp maximum at point 2 (90 kV/cm), indicating the field at which most ferroelastic domains switched from approximately anti-parallel to

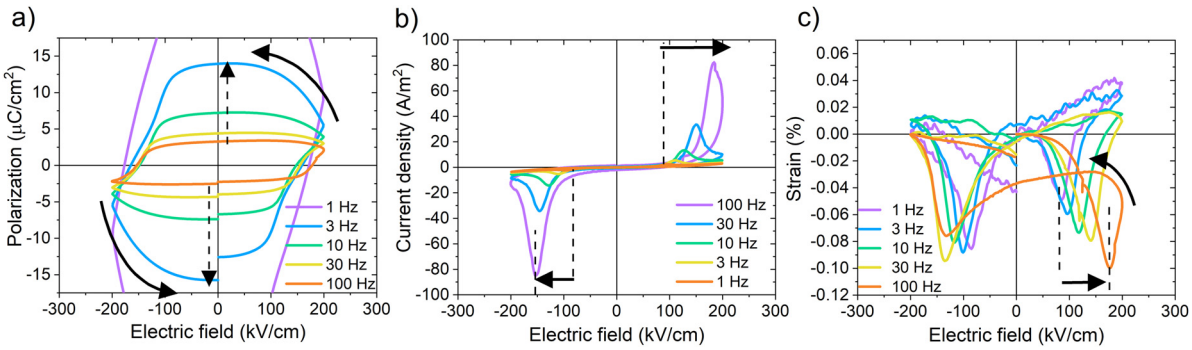

FIG. 3. Hysteresis loops with an electric field amplitude of 200 kV/cm and frequencies of 1, 3, 10, 30, and 100 Hz. (a) Polarization, arrows highlight increasing leakage contributions. (b) Current density, dashed lines mark E_c at 1 and 100 Hz and arrows show the increase. (c) Strain, dashed lines mark E_c at 1 and 100 Hz and arrow shows increase. Curved arrow highlights asymmetry at 100 Hz.

approximately perpendicular to the electric field. From point 2 to 3, the strain rate increased rapidly from −0.002% to 0% s^{-1}, with 0% s^{-1} strain rate corresponding with the minimum in the S–E loop. When the strain rate became positive, the material was expanding and reached a maximum rate at point 3 (130 kV/cm), where the most domains were switching from approximately perpendicular to parallel to the electric field. The strain rate then decreased to near 0% s^{-1} at the maximum electric field (point 4). After maximum electric field strain loops exhibited minor strain recovery from 0.02% to zero during which time the strain rate first went slightly negative, suggestive of back switching but was then effectively 0% s^{-1} until point 5 at 0 kV/cm. This near 0% s^{-1} strain rate signified that very little back switching of domains occurred until the electric field direction was reversed. Due to the high degree of symmetry in the loop, the behavior described between points 1 and 5 is also reflected by the loop between points 5 and 9 in Fig. 2(i).

Two notable observations were made in the strain rate hysteresis as a function of field amplitude. First, for field amplitudes between 100 and 170 kV/cm the strain rate intensity increased, indicating that an increasing portion of ferroelastic domains was being switched with each successive field increase. Second, at field amplitudes from ≥170, the strain rate peaks remained at approximately the same electric field position (130 kV/cm) and the intensities decreased. This indicated that the bulk of ferroelastic domains switched at 130 kV/cm, but that less domains switched at that field as the amplitude was increased. As the S_{pp} ≥170 kV/cm was constant [Fig. 2(f)], the conclusion is that approximately the same total number of ferroelastic domains must switch but distributed over fields between 170 and 260 kV/cm. Such a distribution of switching must result from the rate of electric field increase, which increased with field amplitude, thus revealing a kinetic limit to ferroelastic domain switching.[18–20]

The hysteresis behavior at a field amplitude of 200 kV/cm observed at field frequencies between 1 and 100 Hz provided further insight into the switching kinetics (Fig. 3). The leakage current contribution to P–E hysteresis increased almost exponentially as the frequency decreased [Fig. 3(a)], and the E_c decreased markedly [Fig. 3(b)]. The E_c reduction was also seen in the S–E hysteresis loops, but most notable was the asymmetry in the S–E loop at 100 Hz which indicated incomplete domain switching [Fig. 3(c)].[10] This indication of incomplete switching at 100 Hz correlated well with the kinetic limit revealed by the strain rate analysis. Similarly prepared $[N(CH_3)_4][FeBrCl_3]$ followed domain growth limited-switching described by the Kolmogorov–Avrami–Ishibashi model and was heavily influenced by the presence of charge defect complexes that resulted in a reversible asymmetrical hysteresis at 100 Hz.[10,18] Similarly, defect complexes are considered to play an important role here and evidence for this was also seen in the E_{bias} behavior.

The dielectric response of the material was studied as a function of direct current (DC) bias field to observe the dielectric properties and gain further insight into the domain switching. For these measurements, a small alternating current (AC) signal of 5 kV/cm and 1 kHz frequency was used to measure the dielectric permittivity (relative permittivity, ε_r) and loss, while a sample was subject to a direct current (DC) electric field bias. The bias was increased and decreased in increments first in the positive, and then negative field directions so that the data can be plotted as a permittivity hysteresis loop (Fig. 4). The cycle was repeated several times, increasing the maximum electric field by 10 kV/cm with each successive cycle, but the maximum DC bias field was limited to 120 kV/cm due to sample arcing. For DC bias fields up to 50 kV/cm, the ε_r vs DC bias field loop had a V-like shape and increased linearly from 16.9 at 0 kV/cm in both positive and negative field directions [Fig. 4(a)]. As the DC bias field was increased above 50 kV/cm, peaks in ε_r occurring below the maximum DC bias field emerged. The intensity of ε_r peaks increased as the maximum DC bias field was increased, likely arise from coincidental switching of ferroelectric (180°) and ferroelastic (non-180°) domains, analogously with metal oxide ferroelectrics such as PZT.[21–23] This ε_r peak, while corresponding to domain switching, just like the E_c from the hysteresis

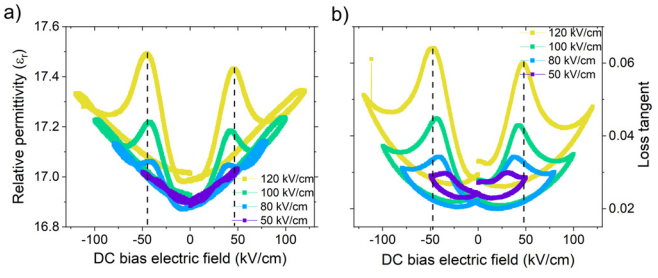

FIG. 4. (a) Relative permittivity and (b) loss tangent, as a function of DC electric field bias up to 120 kV/cm. Dashed lines mark the E_c in the 120 kV/cm DC bias field cycle.

measurements in Figs. 2 and 3, occurred at the much lower field of 45 kV/cm, mostly due to the vastly different electric field conditions for the permittivity measurement. Interestingly however, the underlying V-shape of the ε_r curve was contrary to the behavior observed in metal oxide ferroelectrics, where ε_r decreases below the value at zero DC bias after the maximum ε_r is reached, due to reduced domain wall contributions and internal stress.[21,22] The mechanism for the underlying V-shape behavior observed in the $[N(CH_3)_4][FeBrCl_3]$ is unknown and warrants further investigation, but does bare some similarities with the dielectric response of the classic molecular piezoelectric material Rochelle salt.[24] The corresponding loss tangents had a similar shape and fluctuated between 0.020 and 0.065 [Fig. 4(b)].

In total, the ε_r varied between 16.9 and 17.5 for DC bias up to 120 kV/cm, revealing a low dielectric tunability of 0.035% or 3.5%. By comparison, commercial metal oxide ferroelectric PZT can show tunability of 0.68 over the same field range, thus the plastic crystals $[N(CH_3)_4][FeBrCl_3]$ seem to exhibit rather high dielectric stability as a function of electric field bias.[21–23]

Polycrystalline plastic crystal ferroelectric $[N(CH_3)_4][FeBrCl_3]$ was driven with bipolar electric field amplitudes up to 260 kV/cm, demonstrating a maximum peak-to-peak strain of 0.1%. The hysteresis behavior suggested that ferroelastic domain switching saturated at 170 kV/cm. However, at higher field amplitudes, the rate of electric field increase was too fast for domain switching to keep up, producing a ferroelastic domain switching lag that distributed the strain over higher fields and reduced the maximum strain rate. This kinetic limit of switching was confirmed by hysteresis measurements at 100 Hz that were asymmetric due to incomplete switching. High leakage currents were evident in the polarization and current density hysteresis and were thus expected to play a role in the switching behavior. The dielectric constant and loss tangents under DC bias electric fields also showed domain switching but exhibited a low dielectric tunability of 0.035 with no sign of dielectric stiffening, a finding that warrants further investigation. The observed domain switching dynamics of $[N(CH_3)_4][FeBrCl_3]$ suggest that electric field conditions play an important role in the electromechanical response of these materials. Further detailed studies of additional plastic crystals are needed to reveal universal traits of their ferroelectricity as well as the key differences from metal oxides and will be beneficial to the development of the wider family of supramolecular ferroelectrics.

J.W. and M.A.E. acknowledge the financial support of NTNU.

DATA AVAILABILITY

The data that support the findings of this study are available within the article and upon request from the corresponding author.

REFERENCES

[1]C. R. Bowen, H. A. Kim, P. M. Weaver, and S. Dunn, Energy Environ. Sci. **7**, 25 (2014).
[2]D. Damjanovic, P. Muralt, and N. Setter, IEEE Sens. J. **1**, 191 (2001).
[3]A. Al-Fuqaha, M. Guizani, M. Mohammadi, M. Aledhari, and M. Ayyash, IEEE Commun. Surv. Tutorials **17**, 2347 (2015).
[4]B. Hammi, R. Khatoun, S. Zeadally, A. Fayad, and L. Khoukhi, IET Networks **7**(1), 1 (2018).
[5]S. A. Wilson, R. P. J. Jourdain, Q. Zhang *et al.*, Mater. Sci. Eng. R **56**, 1 (2007).
[6]A. S. Tayi, A. Kaeser, M. Matsumoto, T. Aida, and S. I. Stupp, Nat. Chem. **7**, 281 (2015).
[7]J. Harada, N. Yoneyama, S. Yokokura, Y. Takahashi, A. Miura, N. Kitamura, and T. Inabe, J. Am. Chem. Soc. **140**, 346 (2018).
[8]Z. Czapla, O. Czupinski, Z. Galewski, and L. Sobczyk, Solid State Commun. **56**, 741 (1985).
[9]J. Salgado-Beceiro, S. Castro-Garcia, M. Sanchez-Andujar, and F. Rivadulla, J. Phys. Chem. C **122**, 27769 (2018).
[10]J. Walker, R. Miranti, S. L. Skjærvø, T. Rojac, T. Grande, and M.-A. Einarsrud, J. Mater. Chem. C **8**, 3206–3216 (2020).
[11]H. Yan, F. Inam, G. Viola, H. Ning, H. Zhang, Q. Jiang, T. Zeng, Z. Gao, and M. J. Reece, J. Adv. Dielectr. **1**, 107 (2011).
[12]T. Schenk, E. Yurchuk, S. Mueller, U. Schroeder, S. Starschich, U. Bottger, and T. Mikolajick, Appl. Phys. Rev. **1**, 041103 (2014).
[13]D. Damjanovic, "Hysteresis in piezoelectric and ferroelectric materials," in *Science of Hysteresis*, edited by G. Bertotti and I. Mayergoyz (Academic Press, Oxford, 2006), Vol. III, pp. 337–465.
[14]G. Viola, T. Saunders, X. Wei, K. B. Chong, H. Luo, M. J. Reece, and H. Yan, J. Adv. Dielectr. **3**, 1350007 (2013).
[15]U. Robels and G. Arlt, J. Appl. Phys. **73**, 3454–3457 (1993).
[16]G. Arlt and H. Neumann, Ferroelectrics **87**, 109 (1988).
[17]M. I. Morozov, M.-A. Einarsrud, J. R. Tolchard, P. Geiger, K. G. Webber, D. Damjanovic, and T. Grande, J. Appl. Phys. **118**, 164104 (2015).
[18]W. Li, Z. Chen, and O. Auciello, J. Phys. D **44**, 105404 (2011).
[19]H. Orihara, S. Hashimoto, and Y. Ishibashi, J. Phys. Soc. Jpn. **63**, 1031 (1994).
[20]A. K. Tagantsev, I. Stolichnov, N. Setter, J. S. Cross, and M. Tsukada, Phys. Rev. B **66**, 214109 (2002).
[21]Y. Masuda and A. Baba, Jpn. J. Appl. Phys., Part 1 **24**, 113 (1985).
[22]N. Uchida and T. Ikeda, Jpn. Appl. Phys., Part 1 **4**, 867 (1965).
[23]C. Ang and Z. Yu, Phys. Rev. B **69**, 174109 (2004).
[24]A. G. Slivka, V. M. Kedyulich, R. R. Levitskii, A. P. Moina, M. O. Romanyuk, and A. M. Guivan, Condens. Matter Phys. **8**, 623–638 (2005).